AMERICAN SOCIETY FOR MICROBIOLOGY | Antimicrobial Agents and Chemotherapy®

ANTIVIRAL AGENTS

Favipiravir Pharmacokinetics in Nonhuman Primates and Insights for Future Efficacy Studies of Hemorrhagic Fever Viruses

Vincent Madelain,[a] Jérémie Guedj,[a] France Mentré,[a] Thi Huyen Tram Nguyen,[a] Frédéric Jacquot,[b] Lisa Oestereich,[c,d] Takumi Kadota,[e] Koichi Yamada,[e] Anne-Marie Taburet,[f] Xavier de Lamballerie,[g,h] Hervé Raoul[b]

IAME, UMR 1137, INSERM, Université Paris Diderot, Sorbonne Paris Cité, Paris, France[a]; Laboratoire P4 INSERM-Jean Mérieux, US003 INSERM, Lyon, France[b]; Bernhard Nocht Institute for Tropical Medicine, Hamburg, Germany[c]; German Center for Infection Research (DZIF), Partner Site, Hamburg, Germany[d]; Department of Research Laboratory of Toyama Chemical Co., Ltd., Tokyo, Japan[e]; Hopital Bicêtre, Assistance Publique-Hôpitaux de Paris, INSERM U1184, Center for Immunology of Viral Infections and Autoimmune Diseases, CEA, Université Paris-Sud, Kremlin Bicêtre, Paris, France[f]; UMR Emergence des Pathologies Virales (Aix-Marseille University-IRD 190-INSERM 1207-EHESP), Marseille, France[g]; Institut Hospitalo-Universitaire Méditerranée Infection, Marseille, France[h]

ABSTRACT Favipiravir is an RNA polymerase inhibitor that showed strong antiviral efficacy *in vitro* and in small-animal models of several viruses responsible for hemorrhagic fever (HF), including Ebola virus. The aim of this work was to characterize the complex pharmacokinetics of favipiravir in nonhuman primates (NHPs) in order to guide future efficacy studies of favipiravir in large-animal models. Four different studies were conducted in 30 uninfected cynomolgus macaques of Chinese ($n = 17$) or Mauritian ($n = 13$) origin treated with intravenous favipiravir for 7 to 14 days with maintenance doses of 60 to 180 mg/kg of body weight twice a day (BID). A pharmacokinetic model was developed to predict the plasma concentrations obtained with different dosing regimens, and the model predictions were compared to the 50% effective concentration (EC_{50}) of favipiravir against several viruses. Favipiravir pharmacokinetics were described by a model accounting for concentration-dependent aldehyde oxidase inhibition. The enzyme-dependent elimination rate increased over time and was higher in NHPs of Mauritian origin than in those of Chinese origin. Maintenance doses of 100 and 120 mg/kg BID in Chinese and Mauritian NHPs, respectively, are predicted to achieve median trough plasma free concentrations above the EC_{50} for Lassa and Marburg viruses until day 7. For Ebola virus, higher doses are required. After day 7, a 20% dose increase is needed to compensate for the increase in drug clearance over time. These results will help rationalize the choice of dosing regimens in future studies evaluating the antiviral effect of favipiravir in NHPs and support its development against a variety of HF viruses.

KEYWORDS favipiravir, population pharmacokinetics, hemorrhagic fever, nonhuman primates, modelling

Emerging infectious diseases leading to hemorrhagic fever (HF), with severe prognosis and a strong ability to spread, have become a major public health concern, in particular in countries with limited incomes. Etiologic viruses are diverse and include Ebola virus (EBOV) (1), Marburg virus (MARV) (2), dengue virus (3), Junin virus (JUNV) (4), Crimean-Congo hemorrhagic fever virus (CCHFV) (5), Rift Valley fever virus (RVFV) (6), Lassa virus (LASV) (7), and yellow fever virus (YFV) (8). For most of these viruses, there are no curative therapeutics, and treatment essentially relies on supportive care (9).

Received 19 June 2016 **Returned for modification** 7 August 2016 **Accepted** 27 September 2016

Accepted manuscript posted online 10 October 2016

Citation Madelain V, Guedj J, Mentré F, Nguyen THT, Jacquot F, Oestereich L, Kadota T, Yamada K, Taburet A-M, de Lamballerie X, Raoul H. 2017. Favipiravir pharmacokinetics in nonhuman primates and insights for future efficacy studies of hemorrhagic fever viruses. Antimicrob Agents Chemother 61:e01305-16. https://doi.org/10.1128/AAC.01305-16.

Address correspondence to Vincent Madelain, vincent.madelain@inserm.fr.

TABLE 1 *In vitro* favipiravir antiviral activity against several hemorrhagic fever viruses obtained by virus titer reduction assays on Vero cells

Virus	Strain	EC_{50} (μg/ml)	EC_{90} (μg/ml)[a]	Reference
MARV	Leiden	6.8	11.4	—[b]
RVFV	MP-12	5	ND	17
JUNV	Candid 1	0.79	ND	17
JUNV	Romero	1.9	3.3	17
LASV	Ba366	4.6	6.8	13
LASV	Josiah	1.7–11.1	1.7–11.1	15
CCHFV	Afg-09 2990	1.1	1.2–4.7	12
EBOV	Mayinga 1976	10.5	17.3	11
EBOV	Kikwit 1995/E718	31–63	31–63	16
YFV	17D	42.4	51.8	18

[a]ND, not determined.
[b]See the supplemental material.

Considering the etiologic diversity of these HFs and the fact that they do not represent a major interest for pharmaceutical companies, it is particularly relevant to identify drugs with broad-spectrum activity. Favipiravir, a pyrazine carboxamide derivative initially developed and approved for treatment against resistant influenza in Japan (10), is a relevant candidate, with several studies demonstrating its effectiveness against different HF viruses *in vitro* and in rodent models (10–18). This molecule is an RNA polymerase inhibitor, metabolized intracellularly into the active form favipiravir ribosyl triphosphate, which is thought to prevent viral RNA strand extension and induce lethal mutagenesis (10). Drug efficacy against EBOV was recently evaluated in a clinical trial in Guinea (JIKI trial). The conclusion of this study was that favipiravir monotherapy merits further investigation in patients with low- to medium-level viremia but not in those with high-level viremia (19).

In order to further evaluate the efficacy of this drug, nonhuman primates (NHPs) remain the most relevant animal model for these infections (20). However, experiments

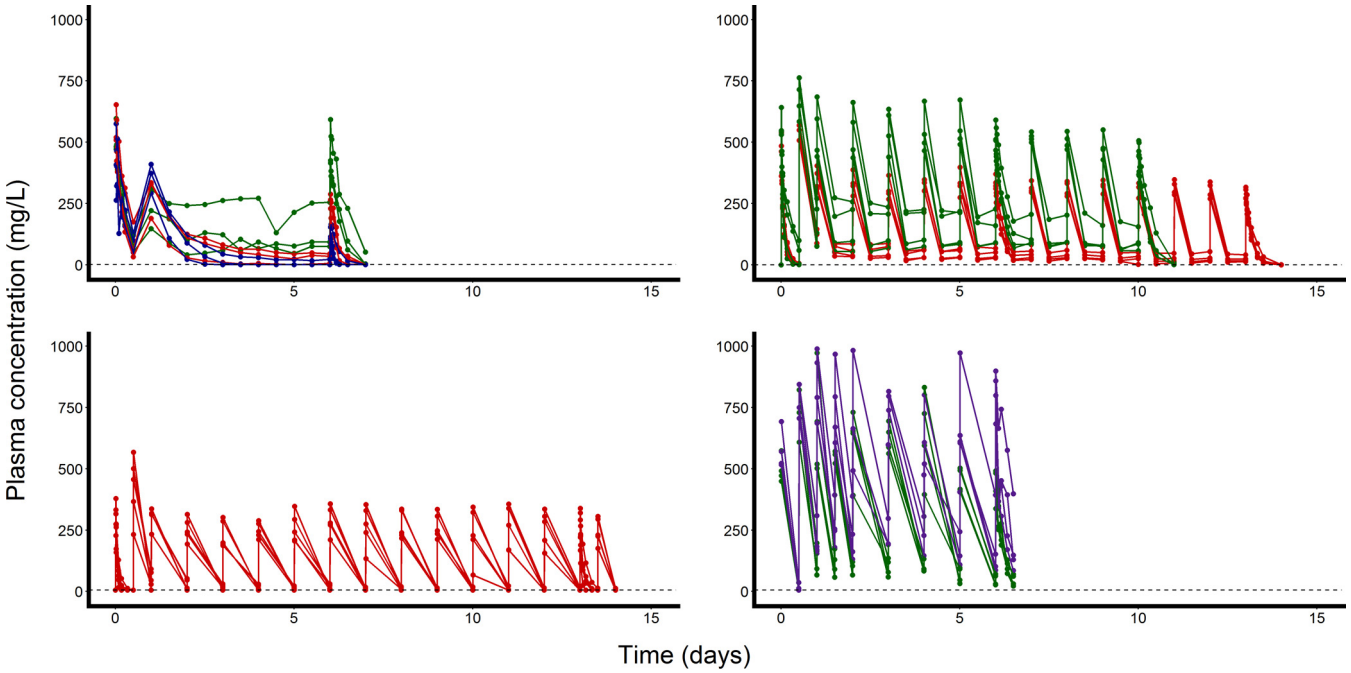

FIG 1 Individual observed pharmacokinetic profiles of favipiravir from study 1A (top left), study 1B (top right), study 2A (bottom left), and study 2B (bottom right). Study 1A included nonanesthetized male Chinese cynomolgus macaques treated for 7 days, study 1B included anesthetized female Chinese cynomolgus macaques treated for 14 days, study 2A included anesthetized female Mauritian cynomolgus macaques treated for 14 days, and study 2B included anesthetized female Mauritian cynomolgus macaques treated for 7 days. Pharmacokinetic profiles for macaques receiving a maintenance dose of 60 mg/kg BID are represented in blue, those for macaques receiving 100 mg/kg BID are in red, those for macaques receiving 150 mg/kg BID are in green, and those for macaques receiving 180 mg/kg BID are in purple. Dashed lines represent the limit of quantification.

TABLE 2 Noncompartmental analysis of favipiravir pharmacokinetic studies in cynomolgus macaques[a]

Study	No. of animals	Loading dose (mg/kg BID)	Maintenance dose (mg/kg BID)	Median C_{trough} (mg/liter) (min–max)			Median C_{max} (mg/liter) (min–max)
				Day 1	Day 7	Day 14	Day 1
1A	3	300	150	76.5 (51.2–120.0)	97.4 (61.8–231.0)	NA	482.0 (472–597)
	3	300	100	58.6 (32.9–175.0)	24.3 (2.8–35.5)	NA	520 (508–653)
	3	300	60	98.9 (51.1–127.0)	BLQ (BLQ–15.7)	NA	408.0 (327.0–575.0)
1B	4	250	150	31.2 (0.5–99.3)	105.6 (68.4–178.0)	56.8[b] (34.2–130.0)	545.0 (531.0–642.0)
	4	200	100	3.3 (0.6–5.5)	30.9 (17.8–52.8)	11.6 (7.1–32.9)	473.5 (362.0–539.0)
2A	5	200	100	BLQ (BLQ–5.8)	9.7 (BLQ–18.1)	10.3 (BLQ–37.3)	316.2 (227.9–378.9)
2B	4	250	180	10.4 (BLQ–35.9)	138.8 (85.4–397.8)	NA	546.1 (515.8–692.1)
	4	250	150	BLQ (BLQ–8.4)	46.0 (21.8–70.5)	NA	481.8 (449.8–573.7)

[a]Medians (minima to maxima) for each parameter for the different studies are shown. Study 1A included nonanesthetized male Chinese cynomolgus macaques treated for 7 days, study 1B included anesthetized female Chinese cynomolgus macaques treated for 14 days, study 2A included anesthetized female Mauritian cynomolgus macaques treated for 14 days, and study 2B included anesthetized female Mauritian cynomolgus macaques treated for 7 days. BLQ, below the limit of quantification; NA, not available.

[b]Noncompartmental parameters were calculated at day 11 due to premature dosing interruption.

are limited by infectious hazards, cost, and ethical issues, which restrain the possibility of conducting large dose-ranging studies with detailed pharmacological assessments. In the case of favipiravir, a drug with complex nonlinear pharmacokinetics (PK) (21) and for which the range of 50% effective concentrations (EC_{50}) against HF viruses is large (Table 1), an additional difficulty is to identify the relevant dosing regimen.

Here we analyzed the PK of intravenous (i.v.) favipiravir in cynomolgus macaques after administration of repeated doses. Based on the results of four studies, we modeled the dose concentration relationship of favipiravir using a population approach, taking into account effects of drug nonlinearity, sex, anesthesia, and geographic origin. Using this model, we performed simulation studies to estimate the impact of various dosing regimens on favipiravir exposure and compared these data with EC_{50} for several HF viruses.

RESULTS

Safety. No animals died, and no toxic effect was found upon necropsy. Transient lacks of feces, vomiting, and stereotypic movement disorders (repeated backward head movements) were noted. A drop in the hemoglobin blood level, associated with an increased reticulocyte count, was observed in the four studies, with median (minimum, maximum) variations of −2.3 g/dl (−0.8, −3.2 g/dl) and −1.3 g/dl (0.2, −4 g/dl) from baseline to day 7 in studies 1A and 2B, respectively, and −2.3 g/dl (−1.4, −2.8 g/dl) and −2 g/dl (−0.9, −2.5 g/dl) from baseline to day 14 in studies 1B and 2A, respectively. In study 1B, in macaques receiving 150 mg/kg twice a day (BID), food consumption decreased continuously during the dosing period, leading to dosing discontinuation on day 11. However, there were no abnormalities in body weights, serum electrolyte concentrations, or general status. In the study 2A macaques receiving 100 mg/kg BID, a moderate increase of the creatinine concentration (+18.6 μmol/liter) was observed at the end of the follow-up period. However, this biological abnormality was not found in groups receiving higher doses of 150 and 180 mg/kg BID. In conclusion, no serious abnormalities were observed with the different dose regimens explored in the four studies. More details can be found in the supplemental material.

Noncompartmental analysis. The data produced in the four PK studies are displayed in Fig. 1. The results showed a strong nonlinearity of favipiravir over doses and time in Chinese cynomolgus macaques in studies 1A and 1B (Table 2). Clearance at day 7 decreased with dose, from 0.13 liters/h/kg to 0.04 liters/h/kg for doses of 60 mg/kg BID to 150 mg/kg BID, respectively. Data from study 1B also showed nonlinearity over time, with an 80% decrease in the clearance rate between day 1 and day 7, occurring from the second administration, and then a 25% increase in the clearance rate between days 7 and 14, for the two levels of maintenance doses.

TABLE 2 (Continued)

Median C_{max} (mg/liter) (min–max)		Median C_{ave} (mg/liter) (min–max)			Median CL (liters/h/kg) (min–max)		
Day 7	Day 14	Day 1	Day 7	Day 14	Day 1	Day 7	Day 14
425 (415–593)	NA	244.1 (222.2–263.2)	240.7 (210.6–358.2)	NA	0.10 (0.10–0.11)	0.05 (0.03–0.06)	NA
265.0 (229.0–288.0)	NA	223.1 (187.9–351.3)	110.9 (61.1–117.8)	NA	0.11 (0.07–0.13)	0.08 (0.07–0.14)	NA
115.0 (106.0–165.0)	NA	203.5 (189.9–309.9)	23.6 (18.0–73.9)	NA	0.12 (0.08–0.13)	0.22 (0.07–0.28)	NA
509.5 (467.0–590.0)	470.5[b] (368.0–506.0)	88.4 (54.3–117.7)	241.4 (214.0–347.6)	194.3[b] (167.3–283.8)	0.25 (0.18–0.38)	0.03 (0.02–0.04)	0.04[b] (0.03–0.05)
328.5 (310.0–370.0)	289.5 (271.0–317.0)	60.3 (51.0–72.9)	131.6 (107.5–159.0)	102.2 (85.3–133.2)	0.28 (0.23–0.33)	0.06 (0.05–0.08)	0.09 (0.06–0.10)
274.8 (133.2–354.0)	291.4 (175.4–339.2)	40.1 (20.9–63.0)	NA	47.9 (16.9–89.9)	0.42 (0.26–0.80)	NA	0.17 (0.09–0.49)
829.2 (683.0–898.7)	NA	NA	368.3 (263.3–626.7)	NA	NA	0.04 (0.02–0.06)	NA
445.9 (337.8–491.9)	NA	NA	187.1 (150.6–217.8)	NA	NA	0.07 (0.06–0.08)	NA

Significantly lower exposure was found in studies 2A and 2B, performed in macaques from Mauritius Island, with a C_{ave} on day 14 of 47.9 mg/liter compared to 102.2 mg/liter for a maintenance dose of 100 mg/kg BID ($P = 0.040$) and a C_{ave} on day 7 of 187.1 mg/liter compared to 241.4 mg/liter for a maintenance dose of 150 mg/kg BID ($P = 0.024$).

PK model building. A one-compartment model with first-order elimination was inadequate to describe the favipiravir PK over 7 days with repeated administrations. The addition of a nonlinear Michaelis-Menten elimination term improved the fit of the data, but it did not allow a description of the concentration increase from the first to the second administrations. Finally, a model including enzyme-mediated elimination with concentration-dependent inhibition provided the best description of the PK profiles of favipiravir, and a combined residual-error model was retained:

$$\frac{dA_c}{dt} = -k \times A_c - k_{\text{enz}} \times A_e \times A_c$$

$$\frac{dA_e}{dt} = R_{\text{in}} - k_{\text{out}} \times (1 + C_c \times \alpha_{\text{deg}}) \times A_e \quad (1)$$

$$R_{\text{in}} = k_{\text{out}} \times A_{e0}$$

$$C_c = \frac{A_c}{V}$$

where A_c is the amount of favipiravir in the central compartment, C_c is the favipiravir plasma concentration, A_e is the enzymatic activity level, k is the first-order elimination rate, k_{enz} is the enzyme-dependent first-order elimination rate, k_{out} is the enzyme elimination rate, R_{in} is the zero-order enzyme synthesis rate, α_{deg} is the linear effect of the favipiravir concentration on the enzyme elimination rate, and V is the volume of distribution. The activity level of the enzyme at baseline, A_{e0}, was set to 1. This model makes the assumption that favipiravir increases enzyme degradation, in accordance with the irreversible inhibition mechanism proposed by the manufacturer.

Next, data from study 1B, where female cynomolgus macaques were treated and anesthetized daily for 14 days, were included. Because the model predicts that the drug rapidly reaches steady state, it could not capture the decrease in drug concentrations between day 7 and day 14. To account for this feature, a time-dependent variation in the enzyme kinetics on α_{deg} was added:

$$\frac{dA_e}{dt} = R_{\text{in}} - k_{\text{out}} \times (1 + C_c \times \alpha_{\text{deg}} \times e^{-\lambda \times t}) \times A_e \quad (2)$$

This model has one additional parameter, λ, which is the rate at which enzyme elimination becomes less and less sensitive to the favipiravir concentration. Thus, with this model, the enzyme activity increases over time and returns to its baseline value, leading to a decrease in the drug concentration. The effect of sex and/or anesthesia was then explored by using this model and selected on k_{out}.

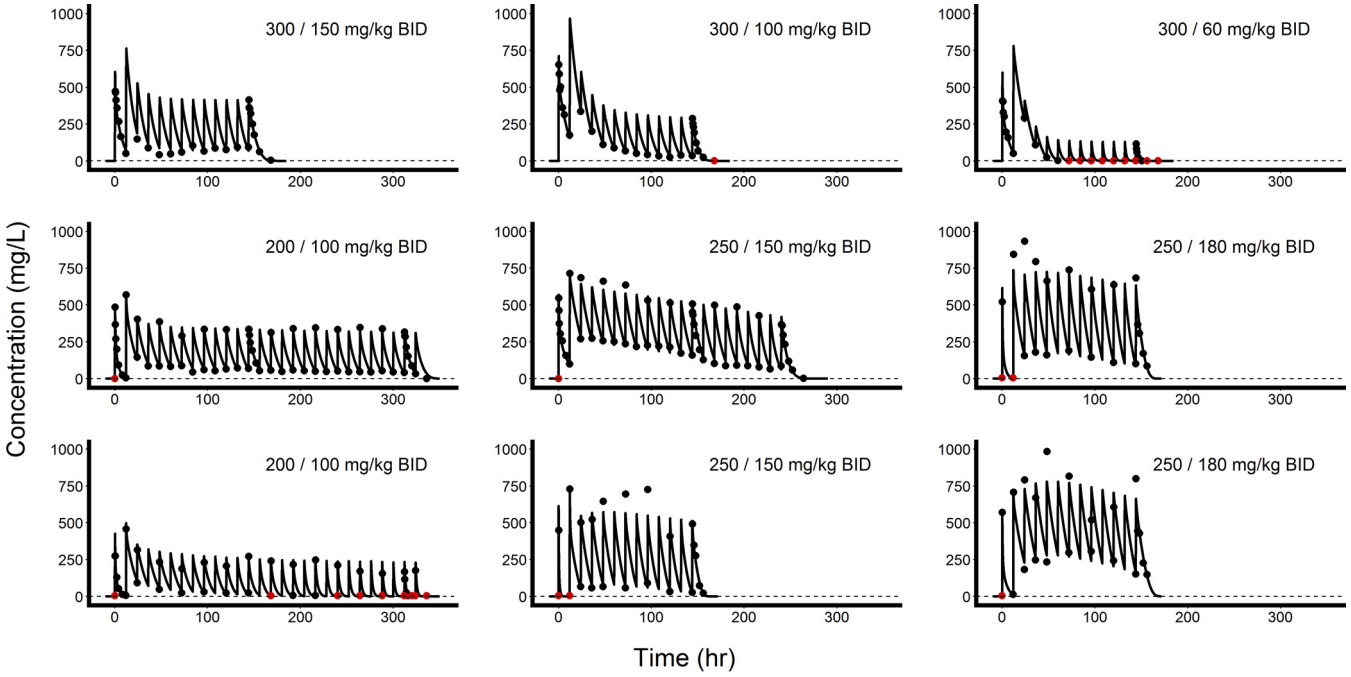

FIG 2 Individual observed concentrations (black dots) and model predictions (solid lines) for macaques treated with various dosing regimens. Red dots indicate data below the limit of quantitation, represented by dashed lines.

Finally, data from studies 2A and 2B were included, and the faster drug elimination in macaques of Mauritian origin was attributed to higher values of k_{enz} and α_{deg} (Table 2). Selection of the random effect led to fixing k_{out} and α_{deg}, and the final model had four independent random effects. Individual fits (see Fig. SA5 in the supplemental material) and diagnostic plots of the final model (Fig. 2; see also Fig. SA6 to SA8 in the supplemental material) did not point out any misspecification.

Model predictions. At the first administration of favipiravir, the enzyme-dependent elimination part is much larger than the independent one, with k_{enz} and k being equal to 2.85 and 0.065 h^{-1}, respectively (Table 3). However, the inhibition of the enzyme by favipiravir leads to a rapid decrease of the enzyme-dependent pathway. The enzyme is continuously synthetized at a rate, R_{in}, equal to 0.024 h^{-1}, and consequently, it takes about 4 days after complete drug elimination to return to the baseline enzyme level. A

TABLE 3 Pharmacokinetic model parameter estimates and associated relative standard errors[a]

Parameter	Estimated fixed effect (RSE, %)	Interindividual variability, ω (%) (RSE, %)
V (liters/kg)	0.359 (2.8)	13.9 (14.5)
k (h^{-1})	0.0654 (6.6)	23.4 (15.2)
k_{enz} for macaques of Mauritian origin (h^{-1})	2.85 (9.8)	24.2 (13.0)
k_{enz} for macaques of Chinese origin (h^{-1})	1.25 (8.8)	
α_{deg} for macaques of Mauritian origin (mg^{-1} liter)	0.179 (10.1)	0 (fixed)
α_{deg} for macaques of Chinese origin (mg^{-1} liter)	0.100 (9.5)	
k_{out} for males (h^{-1})	0.036 (6.4)	0 (fixed)
k_{out} for females (h^{-1})	0.024 (6.0)	
λ (h^{-1})	0.00155 (18.7)	104.1 (16.3)
Residual error		
Additive (mg/liter)	2.77 (7.9)	
Proportional	0.155 (3.1)	

[a]RSE, relative standard error.

sex difference was found for the parameter k_{out}, equal to 0.024 h^{-1} in females and 0.036 h^{-1} in males ($P = 3 \times 10^{-6}$ by a likelihood ratio test [LRT]). In order to fit the decrease in the drug concentration after repeated administration of favipiravir, we estimated λ to be 0.0016 h^{-1} (Table 3). Regarding differences between the two geographic origins, cynomolgus macaques from Mauritius Island had a larger enzyme-dependent elimination constant than did Chinese macaques (k_{enz} equal to 2.85 h^{-1} and 1.25 h^{-1}, respectively; $P = 5 \times 10^{-5}$ by an LRT) and a higher favipiravir concentration linear effect on the enzyme elimination rate (α_{deg} equal to 0.179 and 0.100 liters · mg^{-1}, respectively; $P = 0.0007$ by an LRT). The fact that there is a faster inhibition of the enzyme by favipiravir in Mauritian macaques suggests that the discrepancy in drug concentrations between the two groups might be reduced with high doses.

Simulations with different dosing regimens. Average and residual concentrations were predicted to be lower in Mauritian macaques than in Chinese macaques in all scenarios. At day 7, the average total plasma concentrations in Mauritian (compared to Chinese) cynomolgus macaques were equal to 67 mg/liter (compared to 124 mg/liter), 215 mg/liter (compared to 284 mg/liter), and 312 mg/liter (compared to 384 mg/liter) for maintenance doses of 100, 150, and 180 mg/kg BID, respectively. In order to achieve similarly high concentrations in Mauritian cynomolgus macaques, maintenance doses would need to be equal to 120, 170, and 200 mg/kg BID, respectively (not shown). The loading dose was found to increase concentrations on days 1 and 2 but had a limited impact on enzyme inhibition afterwards (see Table SA1 in the supplemental material). No steady state was reached during the dosing period, and concentrations were predicted to decrease over time, with decreases in the average concentration of 51%, 39%, and 30% between day 7 and day 14 for maintenance doses of 100, 150, and 180 mg/kg BID, respectively, in Mauritian cynomolgus macaques. Increasing the maintenance dose from 100 to 120 mg/kg BID (Chinese-origin macaques) and from 150 to 180 mg/kg BID (Mauritian-origin macaques) on day 7 would allow them to maintain concentrations until day 14 (Fig. 3, middle and right).

Drug exposure and EC_{50} against hemorrhagic fever viruses. In Chinese cynomolgus macaques, the model predicted that a maintenance dose of 100 mg/kg BID may be sufficient to maintain median trough concentrations at day 7 above the EC_{50} of all viruses except EBOV and YFV (Fig. 3). In order to maintain free drug concentrations above the EC_{50} until day 14, the model predicted that an increase in the dose at day 7 from 100 to 120 mg/kg BID is necessary. For EBOV and YFV, higher doses of 150 mg/kg BID until day 7 followed by 180 mg/kg BID afterwards were predicted to maintain free concentrations above the drug EC_{50} until day 14 (Fig. 3, middle).

In Mauritian macaques, the model predicted that a maintenance dose of 150 mg/kg BID may be sufficient to maintain median trough concentrations at all times above the EC_{50} for all viruses except EBOV and YFV (Fig. 3, middle; see also Table SA1 in the supplemental material). In the case of EBOV and YFV, a maintenance dose of 180 mg/kg BID maintains the concentrations above the drug EC_{50} until day 7 but not afterwards (Fig. 3).

DISCUSSION

The pharmacokinetics of favipiravir exhibited nonlinearity over dose and over time, with a marked increase in drug concentrations between the first and second administrations, followed by a progressive reduction afterwards until the end of the dosing period. A model with an enzyme inhibition process was developed to characterize this complex profile, which allowed us to fit the data and to make predictions for a variety of unobserved scenarios.

The complexity of the drug PK and the large variability in drug concentrations across animals are likely due to the fact that favipiravir inhibits aldehyde oxidase, which is the main enzyme involved in the drug elimination (21). This enzyme targets and is inhibited by many molecules *in vitro*, such as raloxifene, menadione, or amitriptyline (27). There are no data to our knowledge on the aldehyde oxidase phenotypes across macaque

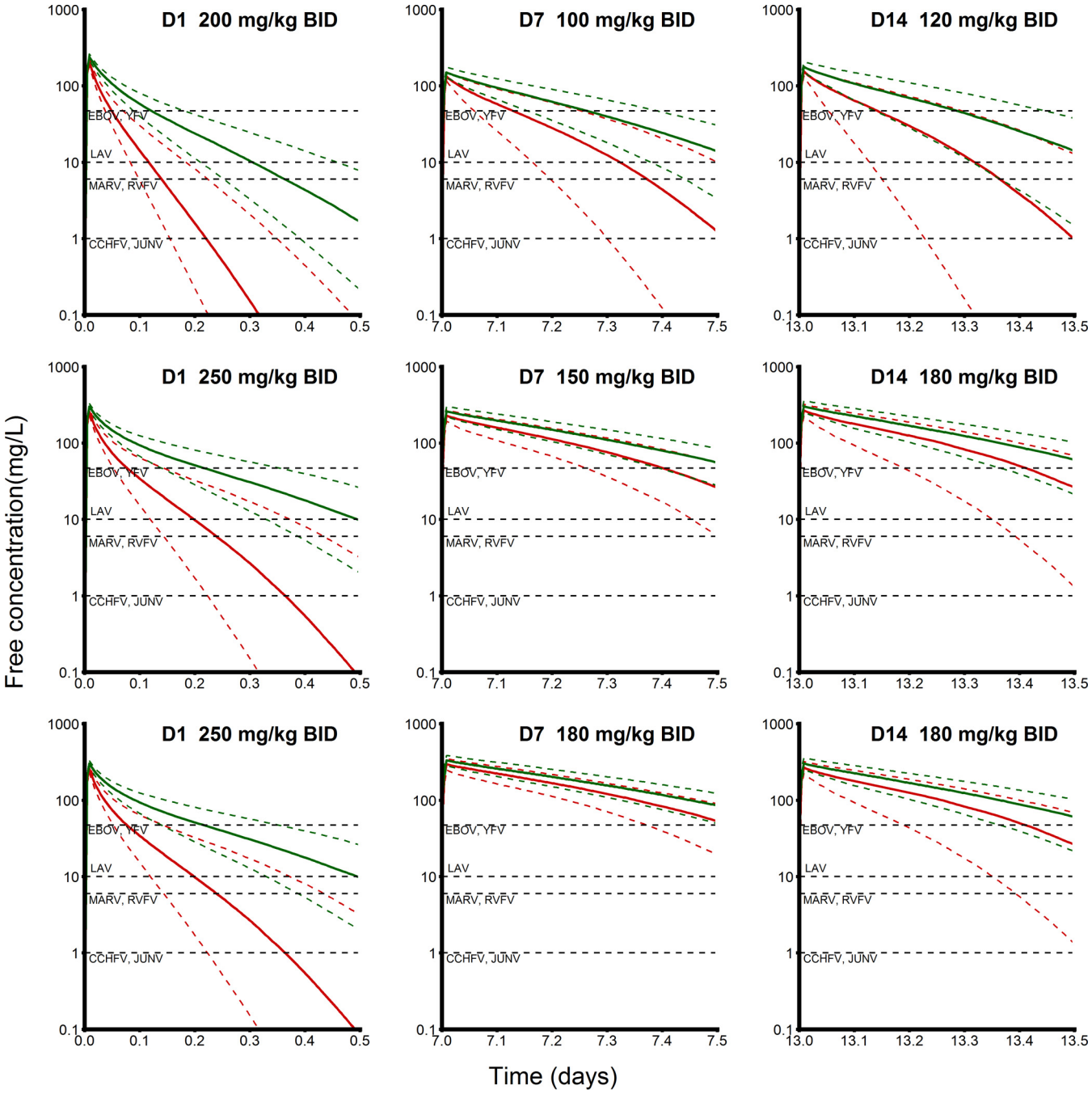

FIG 3 Prediction of plasma free concentrations (assuming a protein binding rate of 50%) of favipiravir in female Chinese (green) and Mauritian (red) cynomolgus macaques on day 1 (left), day 7 (middle), and day 14 (right) with various dosing regimens. (Top) Doses of 200 mg/kg BID on day 1, 100 mg/kg BID on days 2 to 7, and 120 mg/kg on days 8 to 14; (middle) 250 mg/kg BID on day 1, 150 mg/kg BID on days 2 to 7, and 180 mg/kg on day 8 to 14; (bottom) 250 mg/kg BID on day 1 and 180 mg/kg BID on days 2 to 14. For each profile, 1,000 macaques were simulated, and medians (solid lines) and 25th and 75th percentiles (dashed lines) are given. EC_{50} are given in Table 1. EBOV, Ebola virus; YFV, yellow fever virus; LAV, Lassa fever virus; MARV, Marburg virus; RVFV, Rift Valley fever virus; CCHFV, Crimea-Congo hemorrhagic fever virus; JUNV, Junin virus.

populations. However, it is known that Mauritian and Southeast Asian cynomolgus macaque populations have a genetic gap (28, 29), and therefore, it is possible that this genetic difference explains the discrepancy in PK between the two species. Yet, and in spite of efforts to standardize the protocol studies and animal handling, the experiments were performed in two different laboratories, and thus, one cannot rule out that the differences found between the two species are due to confounding factors.

Another intriguing pattern of the drug PK was the decrease in drug concentrations

over time, which was captured by using a time-varying parameter. We also tested a more physiological model with a feedback mechanism where the decrease of the aldehyde oxidase activity due to favipiravir increases enzyme synthesis, but data fitting was not improved. It is noteworthy that a decrease in drug concentrations over time was also found for EBOV-infected patients treated with high doses of favipiravir (unpublished results).

In terms of safety, a decrease in food consumption imputed to favipiravir was observed for the macaques during the dosing period in study 1B at a dose of 150 mg/kg BID, leading to dosing discontinuation on day 11, but not in those in study 2B treated for 7 days with 180 mg/kg BID, which had higher exposure (Table 2). Global impairment of psychomotor activities, including decreases in food intake, was previously reported in an oral-dose toxicity study in Chinese cynomolgus macaques receiving 1,000 mg/kg/day, confirming results for other species showing that high concentrations of favipiravir transiently depress the central nervous system (30). Besides this observation, no other abnormalities in body weights, serum electrolyte concentrations, general condition, or necropsy that required dosing interruption for macaques were reported. Considering the data from the four studies, some biological alterations were noticed, in particular anemia and liver cytolysis (see the supplemental material). These changes were also previously reported in toxicity studies (30), and they were reversible after a 1-month recovery.

In order to simulate drug exposure with different dosing regimens, a number of assumptions were made. First, the studies were conducted in noninfected animals, and infection may alter the drug concentration. For instance, a decrease of the favipiravir concentration was observed in a hamster model of arenavirus hemorrhagic fever (31). Second, the criterion used to propose the dosing regimens was based on the comparison between the EC_{50} observed *in vitro* and the free plasma concentration of favipiravir, which may not be the best marker of nucleoside analogue antiviral activity. Besides, no PK sampling was performed on the tissues to explore favipiravir diffusion. Indeed, the active form of favipiravir is the intracellular triphosphate metabolite (32), which could present different kinetics from the parent form, as was observed for other nucleoside analogues in HIV infection (33). Nonetheless, the half-life of the intracellular triphosphate metabolite, as estimated for human peripheral blood mononuclear cells, is equal to 2 h (30). Although a higher value (5.6 h) was found in influenza virus-infected MDCK cells (34), these values are comparable to the plasma favipiravir half-life, which ranges from 2 h to 6 h, as found in this study and in other contexts (21). Therefore, the PK of the active intracellular metabolite is likely limited by its rate of formation, and it is reasonable to assume that antiviral activity is driven by favipiravir PK. Third, the criterion to find relevant dosing regimens was based on the predose drug concentrations, but average or cumulative exposure may also be relevant. More generally, the exposure-response relationship cannot be anticipated, and a PK-virus dynamic analysis, as proposed, for instance, for mice infected with EBOV (35), will be needed to fully characterize the antiviral activity of favipiravir. In this respect, viral dynamic modeling teaches that the time of treatment initiation is critical to reduce virus levels and that a drug affecting viral replication, such as favipiravir, will have only a very limited impact on viremia if it is administered after peak viremia (35). Furthermore, the duration of treatment may also be critical, as previous studies showed that EBOV-infected macaques treated with BCX4430 or ZMapp may still have detectable viremia at 14 days postchallenge (36, 37). Treatment duration and exposure can also in theory affect the emergence of resistance. Although there is no evidence so far of resistance to favipiravir in influenza or HF viruses (10, 38), the emergence of resistant Chikungunya mutants consecutive to low-level exposure to favipiravir in cellular culture was reported (39). Therefore, it cannot be ruled out that treatment duration, in particular if drug concentrations decline over time, may increase the risk of emergence of resistance.

In conclusion, we developed a mathematical model to predict plasma exposure to favipiravir in NHPs with various dosing regimens. This information can be used to

design studies evaluating favipiravir efficacy and to characterize the dose-response relationship of favipiravir against a variety of viruses responsible for HF.

MATERIALS AND METHODS

Four studies of uninfected cynomolgus macaques were conducted to determine the PK of favipiravir (Fig. 1). Studies 1A and 1B were conducted by the manufacturer, Toyama Chemicals Ltd., in Japan on macaques from China. Studies 2A and 2B were conducted by Silabe and Eurofin/ADME Bioanalyses in France, on behalf of the academic European Reaction Consortium, on macaques from Mauritius Island. The Toyama study protocols were written in accordance with the animal welfare bylaws of Shin Nippon Biomedical Laboratories DSR and reviewed by the Institutional Animal Care and Use Committee (approval no. 2014-0662 and IACUC063-073). Reaction studies were approved by the French Research Ministry (approvals 02015011614462849 and 2015062511215426V1) after favorable opinion of the C2EA35-CREMEAS ethic committee.

Drug administration. In the four studies, favipiravir was dissolved in water for injection to a final concentration of 50 mg/ml after being added with an equivalent molar mass of meglumine. Favipiravir was then diluted with physiological saline on the day of or the day before dosing to give 40-, 30-, and 20-mg/ml formulations, which were administered to macaques by short intravenous infusion. In order to mimic infection studies, animals in studies 1B, 2A, and 2B were anesthetized within 30 min before each drug administration by intramuscular injection of 2.5 mg/kg of body weight tiletamine hydrochloride salt–2.5 mg/kg zolazepam hydrochloride salt (Zoletil). Favipiravir was administered without anesthesia in study 1A. In the four studies, venous access for drug administration was distinct from venous access for sampling to prevent any contamination.

Study design. Study 1A was a 1-week repeated-i.v.-dose PK study including nine nonanesthetized male cynomolgus macaques from China (5 to 7 years old, weighing 5.1 to 7.9 kg). All macaques received the same loading dose of 300 mg/kg BID on day 1, followed by a maintenance dose of 150 mg/kg ($n = 3$), 100 mg/kg ($n = 3$), or 60 mg/kg ($n = 3$) BID every 12 h by a short infusion of 20 min. Drug concentrations were measured frequently on day 1 and day 7 (before dosing, 5 and 30 min and 1, 2, 4, 6, and 12 h after dosing, and 24 h after dosing on day 7) and twice a day before dosing between day 2 and day 6.

Study 1B was a 2-week repeated-i.v.-dose PK study including eight female anesthetized cynomolgus macaques from China (4 to 5 years old, weighing 3.3 to 4.3 kg). Macaques received a loading dose of either 200 mg/kg BID on day 1, followed by a maintenance dose of 100 mg/kg BID ($n = 4$), or 250 mg/kg BID on day 1, followed by a maintenance dose of 150 mg/kg BID ($n = 4$), every 12 h by a short infusion of 10 min. Drug concentrations were measured frequently on day 1, day 7, and day 14 (before dosing, 5 and 20 min and 1, 2, 4, 8, and 12 hours after dosing, 5 min after the second dosing on day 1 and day 7, and 24 h after dosing on day 14) and three times a day on the other days (before dosing, 5 min after dosing, and before the second dosing).

Study 2A was a 2-week repeated-i.v.-dose PK study including five female anesthetized cynomolgus macaques from Mauritius Island (3.8 to 3.9 years old, weighing 3.5 to 4.8 kg). All macaques received a loading dose of 200 mg/kg BID on day 1, followed by a maintenance dose of 100 mg/kg BID every 12 h by a short infusion of 10 min. Drug concentrations were frequently measured on day 1 and day 14 (before dosing; 5 min, 20 min, 2 h, 4 h, 8 h, and 12 h after dosing; 5 min after the second dosing; and 24 h after the second dosing on day 14) and two times a day on the other days (before the second dosing and 5 min after the second dosing).

Study 2B was a 1-week repeated-i.v.-dose PK study including eight female anesthetized cynomolgus macaques from Mauritius Island (3.4 to 4.7 years old, weighing 3.6 to 4.8 kg). Macaques received a loading dose of either 250 mg/kg BID on day 1, followed by a maintenance dose of 150 mg/kg BID ($n = 4$), or 250 mg/kg BID on day 1, followed by a maintenance dose of 180 mg/kg BID ($n = 4$) every 12 h by a short infusion of 10 min. Drug concentrations were measured frequently on day 7 (before dosing and 5 min, 2 h, 4 h, 8 h, and 12 h after dosing), four times a day on day 1 and day 2 (before and 5 min after the first and second dosings), and three times a day on the other days (before and 5 min after the first dosing and before the second dosing).

Safety. Clinical signs, body weight, and food consumption were assessed daily. Hematology and blood chemistry parameters, including hemoglobin concentrations; red cell, white cell, and platelet counts; reticulocyte counts; and serum creatine kinase, aspartate transaminase (AST), alanine aminotransferase (ALT), bilirubin, creatinine, nitrogen urea, sodium, potassium, chlorine, and calcium levels, were assayed in the pretreatment period and at the end of the follow-up period. All animals were euthanized on the last day of the study and necropsied in studies 1B, 2A, and 2B but not in study 1A.

Analysis methods and cross-validation of data from favipiravir concentration assays. Favipiravir plasma concentrations were assayed separately in studies 1 and 2 by using high-performance liquid chromatography (HPLC) coupled to UV detection (Shimadzu 10A and SPD 10A, respectively) and HPLC coupled to tandem mass spectrometry detection (Kromasil C_{18} and API4000, respectively), respectively, with limits of quantification (LOQs) of 0.1 mg/liter and 5 mg/liter, respectively. Cross-validation of the two analytical processes was performed on 15 samples in a blind fashion (see the supplemental material).

Noncompartmental analysis. For each animal, the maximal concentration of drug in serum (C_{max}); the predose concentration (C_{trough}); the average concentration (C_{ave}), defined as the area under the concentration-time curve from 0 to 12 h (AUC_{0-12}) divided by 12; and the clearance rate (CL), defined as dose/AUC, were obtained by noncompartmental approaches after the first administrations on day 1, day 7, and/or day 14 (see the supplemental material). Medians and ranges for parameters in each study were reported, and Wilcoxon tests were used for statistical comparisons between groups.

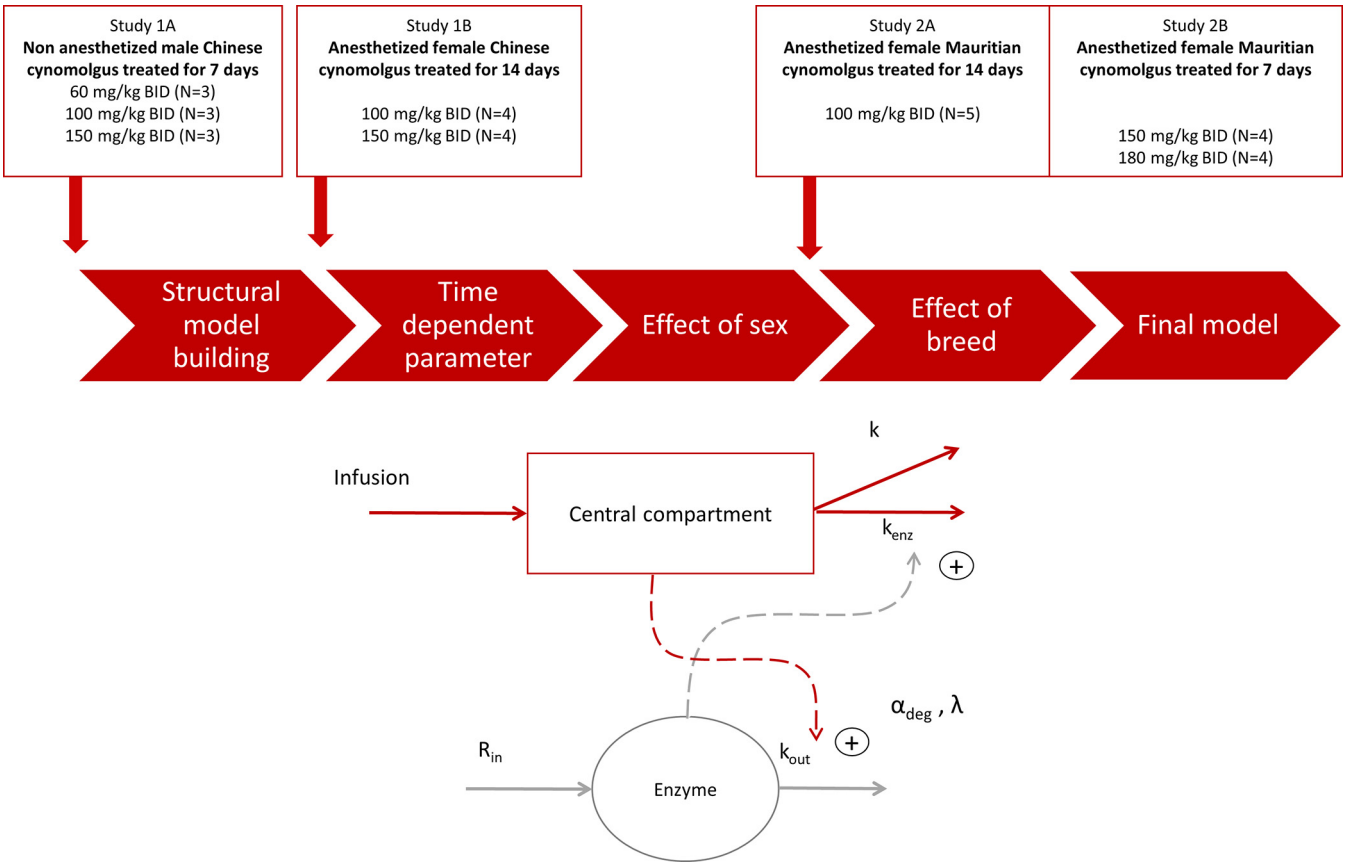

FIG 4 Strategy used to build the pharmacokinetic model (top) and final pharmacokinetic model of favipiravir in cynomolgus macaques (bottom). Parameter k is the enzyme-independent elimination rate constant, k_{enz} is the enzyme-dependent elimination rate, R_{in} is the zero-order enzyme synthesis rate, k_{out} is the one-order elimination rate, and α_{deg} is the linear effect of the favipiravir concentration on the enzyme elimination constant.

Modeling favipiravir pharmacokinetics in cynomolgus macaques. A PK model of favipiravir concentrations in cynomolgus macaques was developed by using the strategy depicted in Fig. 4.

Pharmacokinetic and residual-error models were selected by using data from the 1-week study 1A. We started with a monocompartmental model with linear elimination. Because nonlinearity was observed in the noncompartmental analysis (see Results), we also tested a model with a Michaelis-Menten elimination, a model with both zero-order and first-order eliminations, a model with both first-order and Michaelis-Menten eliminations, and a model with both first-order and nonlinear eliminations depending on favipiravir plasma concentration levels (see equation 1, above), accounting for the aldehyde oxidase pathway. All these models were tested by assuming exponential random effects on all parameters with a diagonal variance matrix for the random effects.

Next, data from study 1B were added; as it was a 2-week study, the time effect was tested on elimination and enzyme parameters. Additions of linear, inverse tangent, and exponential time functions on elimination and enzyme parameters, as well as the feedback effect on enzyme production, were tested. The effect of sex and anesthesia (since the design of the studies does not allow them to be separated) was evaluated. Finally, data from studies 2A and 2B were added, and the parameters were reestimated to assess the effect of NHP origin (China and Mauritius Island for studies 1 and 2, respectively), and relevant random effects were selected.

Model estimation was performed by using a nonlinear mixed-effect model and Monolix 4.2.2 software (Lixoft) (22). Structural, covariate, and residual-error model selections were based on the Bayesian information criterion (BIC) value, a fitting criterion based on the model likelihood that takes into account the number of parameters in the model. Random effects with a variance of <0.1 or associated with a relative standard error of $>100\%$ were deleted by using a backward procedure. Correlations for random effects were added to the final model for parameters presenting Pearson correlation coefficients of >0.6 between their individual predictions. Selection of the covariate effect on structural parameters was performed by using a forward procedure, where the covariate was added sequentially for each parameter. The procedure continued until no improvement in the BIC value was obtained. Maximum likelihood estimation took into account the information brought by data under the LOQ, as described previously (23). Model assessment was performed throughout model building by using diagnostic plots: observations versus population predictions, observations versus individual predictions, individual weighted residuals over time and individual predictions, normalized prediction distribution errors over time and individual predictions, and visual predictive check per dose (24, 25).

Simulation studies with different dosing regimens. We used the final PK model to evaluate by simulation the drug exposure that could be achieved during 2 weeks of favipiravir treatment with a loading dose of 200 or 250 mg/kg BID on the first day followed by a maintenance dose ranging from 60 to 180 mg/kg BID. In order to take into account the possible reduction in drug concentrations over time (see Results), we also evaluated scenarios where the dosing regimen increased in the second week of treatment. For each scenario, 5,000 *in silico* PK profiles with frequent sampling measurements were generated by using the mlxR package (http://simulx.webpopix.org/mlxr/), and daily C_{ave}, C_{trough}, and C_{max} values were provided.

Drug exposure and EC_{50} of favipiravir against hemorrhagic fever viruses. The *in vitro* EC_{50} of favipiravir against a variety of hemorrhagic fever viruses are reported in Table 1. When several EC_{50} were reported in the literature, we chose to be conservative, and only the highest value was considered. We then compared the median predicted drug concentration profiles with the EC_{50} reported in the literature. Consistent with what had been done previously, we relied on free drug concentrations, assuming a protein binding rate of 50% in cynomolgus macaques (unpublished data, Toyama Chemicals Ltd.), close to the value in humans (54%) (26).

For MARV, given that no information was available, cell culture experiments were performed purposely (see the supplemental material). Favipiravir EC_{50} and EC_{90} values were found to be equal to 6.8 and 11.4 μg/ml, respectively, in cell culture experiments (see the supplemental material).

SUPPLEMENTAL MATERIAL

Supplemental material for this article may be found at https://doi.org/10.1128/AAC.01305-16.

TEXT S1, PDF file, 2 MB.

ACKNOWLEDGMENTS

T.K. and K.Y. are employed by Toyama Chemicals, the manufacturer of favipiravir. A.-M.T. declares no conflict of interest.

This project, including the efforts of Vincent Madelain, Jérémie Guedj, France Mentré, Thi Huyen Tram Nguyen, Frédéric Jacquot, Xavier de Lamballerie, and Hervé Raoul, has received funding from the European Union's Horizon 2020 research and innovation program under grant agreement no. 666092 and from Saint Luke University (Japan). L.O. was supported by a grant from the European Commission to evaluate the effect of favipiravir on replication of Marburg virus in cell culture.

REFERENCES

1. Beeching NJ, Fenech M, Houlihan CF. 2014. Ebola virus disease. BMJ 349:g7348. https://doi.org/10.1136/bmj.g7348.
2. van Paassen J, Bauer MP, Arbous MS, Visser LG, Schmidt-Chanasit J, Schilling S, Ölschläger S, Rieger T, Emmerich P, Schmetz C, van de Berkmortel F, van Hoek B, van Burgel ND, Osterhaus AD, Vossen AC, Günther S, van Dissel JT. 2012. Acute liver failure, multiorgan failure, cerebral oedema, and activation of proangiogenic and antiangiogenic factors in a case of Marburg haemorrhagic fever. Lancet Infect Dis 12:635–642. https://doi.org/10.1016/S1473-3099(12)70018-X.
3. Guzman MG, Harris E. 2015. Dengue. Lancet 385:453–465. https://doi.org/10.1016/S0140-6736(14)60572-9.
4. Grant A, Seregin A, Huang C, Kolokoltsova O, Brasier A, Peters C, Paessler S. 2012. Junín virus pathogenesis and virus replication. Viruses 4:2317–2339. https://doi.org/10.3390/v4102317.
5. Ergönül O. 2006. Crimean-Congo haemorrhagic fever. Lancet Infect Dis 6:203–214. https://doi.org/10.1016/S1473-3099(06)70435-2.
6. Ikegami T, Makino S. 2011. The pathogenesis of Rift Valley fever. Viruses 3:493–519. https://doi.org/10.3390/v3050493.
7. Richmond JK, Baglole DJ. 2003. Lassa fever: epidemiology, clinical features, and social consequences. BMJ 327:1271–1275. https://doi.org/10.1136/bmj.327.7426.1271.
8. Monath TP, Vasconcelos PFC. 2015. Yellow fever. J Clin Virol 64:160–173. https://doi.org/10.1016/j.jcv.2014.08.030.
9. Pigott DC. 2005. Hemorrhagic fever viruses. Crit Care Clin 21:765–783. https://doi.org/10.1016/j.ccc.2005.06.007.
10. Furuta Y, Gowen BB, Takahashi K, Shiraki K, Smee DF, Barnard DL. 2013. Favipiravir (T-705), a novel viral RNA polymerase inhibitor. Antiviral Res 100:446–454. https://doi.org/10.1016/j.antiviral.2013.09.015.
11. Oestereich L, Lüdtke A, Wurr S, Rieger T, Muñoz-Fontela C, Günther S. 2014. Successful treatment of advanced Ebola virus infection with T-705 (favipiravir) in a small animal model. Antiviral Res 105:17–21. https://doi.org/10.1016/j.antiviral.2014.02.014.
12. Oestereich L, Rieger T, Neumann M, Bernreuther C, Lehmann M, Krasemann S, Wurr S, Emmerich P, de Lamballerie X, Ölschläger S, Günther S. 2014. Evaluation of antiviral efficacy of ribavirin, arbidol, and T-705 (favipiravir) in a mouse model for Crimean-Congo hemorrhagic fever. PLoS Negl Trop Dis 8:e2804. https://doi.org/10.1371/journal.pntd.0002804.
13. Oestereich L, Rieger T, Lüdtke A, Ruibal P, Wurr S, Pallasch E, Bockholt S, Krasemann S, Muñoz-Fontela C, Günther S. 2016. Efficacy of favipiravir alone and in combination with ribavirin in a lethal, immunocompetent mouse model of Lassa fever. J Infect Dis 213:934–938. https://doi.org/10.1093/infdis/jiv522.
14. Caroline AL, Powell DS, Bethel LM, Oury TD, Reed DS, Hartman AL. 2014. Broad spectrum antiviral activity of favipiravir (T-705): protection from highly lethal inhalational Rift Valley fever. PLoS Negl Trop Dis 8:e2790. https://doi.org/10.1371/journal.pntd.0002790.
15. Safronetz D, Rosenke K, Westover JB, Martellaro C, Okumura A, Furuta Y, Geisbert J, Saturday G, Komeno T, Geisbert TW, Feldmann H, Gowen BB. 2015. The broad-spectrum antiviral favipiravir protects guinea pigs from lethal Lassa virus infection post-disease onset. Sci Rep 5:14775. https://doi.org/10.1038/srep14775.
16. Smither SJ, Eastaugh LS, Steward JA, Nelson M, Lenk RP, Lever MS. 2014. Post-exposure efficacy of oral T-705 (favipiravir) against inhalational Ebola virus infection in a mouse model. Antiviral Res 104:153–155. https://doi.org/10.1016/j.antiviral.2014.01.012.
17. Gowen BB, Wong M-H, Jung K-H, Sanders AB, Mendenhall M, Bailey KW, Furuta Y, Sidwell RW. 2007. In vitro and in vivo activities of T-705 against arenavirus and bunyavirus infections. Antimicrob Agents Chemother 51:3168–3176. https://doi.org/10.1128/AAC.00356-07.
18. Julander JG, Shafer K, Smee DF, Morrey JD, Furuta Y. 2009. Activity of

T-705 in a hamster model of yellow fever virus infection in comparison with that of a chemically related compound, T-1106. Antimicrob Agents Chemother 53:202–209. https://doi.org/10.1128/AAC.01074-08.
19. Sissoko D, Laouenan C, Folkesson E, M'Lebing A-B, Beavogui A-H, Baize S, Camara A-M, Maes P, Shepherd S, Danel C, Carazo S, Conde MN, Gala J-L, Colin G, Savini H, Bore JA, Le Marcis F, Koundouno FR, Petitjean F, Lamah M-C, Diederich S, Tounkara A, Poelart G, Berbain E, Dindart J-M, Duraffour S, Lefevre A, Leno T, Peyrouset O, Irenge L, Bangoura N, Palich R, Hinzmann J, Kraus A, Barry TS, Berette S, Bongono A, Camara MS, Chanfreau Munoz V, Doumbouya L, Harouna S, Kighoma PM, Koundouno FR, Lolamou R, Loua CM, Massala V, Moumouni K, Provost C, Samake N, Sekou C, et al. 2016. Experimental treatment with favipiravir for Ebola virus disease (the JIKI trial): a historically controlled, single-arm proof-of-concept trial in Guinea. PLoS Med 13:e1001967. https://doi.org/10.1371/journal.pmed.1001967.
20. Shurtleff AC, Warren TK, Bavari S. 2011. Nonhuman primates as models for the discovery and development of ebolavirus therapeutics. Expert Opin Drug Discov 6:233–250. https://doi.org/10.1517/17460441.2011.554815.
21. Madelain V, Nguyen THT, Olivo A, de Lamballerie X, Guedj J, Taburet A-M, Mentré F. 2016. Ebola virus infection: review of the pharmacokinetic and pharmacodynamic properties of drugs considered for testing in human efficacy trials. Clin Pharmacokinet 55:907–923. https://doi.org/10.1007/s40262-015-0364-1.
22. Lavielle M. 2014. Mixed effects models for the population approach: models, tasks, methods and tools, p 161–197. CRC Press, Boca Raton, FL.
23. Samson A, Lavielle M, Mentré F. 2006. Extension of the SAEM algorithm to left-censored data in nonlinear mixed-effects model: application to HIV dynamics model. Comput Stat Data Anal 51:1562–1574. https://doi.org/10.1016/j.csda.2006.05.007.
24. Bergstrand M, Hooker AC, Wallin JE, Karlsson MO. 2011. Prediction-corrected visual predictive checks for diagnosing nonlinear mixed-effects models. AAPS J 13:143–151. https://doi.org/10.1208/s12248-011-9255-z.
25. Comets E, Brendel K, Mentré F. 2010. Model evaluation in nonlinear mixed effect models, with applications to pharmacokinetics. J Soc Fr Statistique 151:106–128.
26. Mentré F, Taburet A-M, Guedj J, Anglaret X, Keïta S, de Lamballerie X, Malvy D. 2015. Dose regimen of favipiravir for Ebola virus disease. Lancet Infect Dis 15:150–151. https://doi.org/10.1016/S1473-3099(14)71047-3.
27. Obach RS, Huynh P, Allen MC, Beedham C. 2004. Human liver aldehyde oxidase: inhibition by 239 drugs. J Clin Pharmacol 44:7–19. https://doi.org/10.1177/0091270003260336.
28. Tosi AJ, Coke CS. 2007. Comparative phylogenetics offer new insights into the biogeographic history of Macaca fascicularis and the origin of the Mauritian macaques. Mol Phylogenet Evol 42:498–504. https://doi.org/10.1016/j.ympev.2006.08.002.
29. Ogawa LM, Vallender EJ. 2014. Genetic substructure in cynomolgus macaques (Macaca fascicularis) on the island of Mauritius. BMC Genomics 15:748. https://doi.org/10.1186/1471-2164-15-748.
30. Pharmaceuticals and Medical Devices Agency. 2014. Review report. Pharmaceuticals and Medical Devices Agency, Tokyo, Japan. https://www.pmda.go.jp/files/000210319.pdf.
31. Gowen BB, Sefing EJ, Westover JB, Smee DF, Hagloch J, Furuta Y, Hall JO. 2015. Alterations in favipiravir (T-705) pharmacokinetics and biodistribution in a hamster model of viral hemorrhagic fever. Antiviral Res 121:132–137. https://doi.org/10.1016/j.antiviral.2015.07.003.
32. Furuta Y, Takahashi K, Kuno-Maekawa M, Sangawa H, Uehara S, Kozaki K, Nomura N, Egawa H, Shiraki K. 2005. Mechanism of action of T-705 against influenza virus. Antimicrob Agents Chemother 49:981–986. https://doi.org/10.1128/AAC.49.3.981-986.2005.
33. Bazzoli C, Jullien V, Le Tiec C, Rey E, Mentré F, Taburet A-M. 2010. Intracellular pharmacokinetics of antiretroviral drugs in HIV-infected patients, and their correlation with drug action. Clin Pharmacokinet 49:17–45. https://doi.org/10.2165/11318110-000000000-00000.
34. Smee DF, Hurst BL, Egawa H, Takahashi K, Kadota T, Furuta Y. 2009. Intracellular metabolism of favipiravir (T-705) in uninfected and influenza A (H5N1) virus-infected cells. J Antimicrob Chemother 64:741–746. https://doi.org/10.1093/jac/dkp274.
35. Madelain V, Oestereich L, Graw F, Nguyen THT, de Lamballerie X, Mentré F, Günther S, Guedj J. 2015. Ebola virus dynamics in mice treated with favipiravir. Antiviral Res 123:70–77. https://doi.org/10.1016/j.antiviral.2015.08.015.
36. Warren TK, Wells J, Panchal RG, Stuthman KS, Garza NL, Van Tongeren SA, Dong L, Retterer CJ, Eaton BP, Pegoraro G, Honnold S, Bantia S, Kotian P, Chen X, Taubenheim BR, Welch LS, Minning DM, Babu YS, Sheridan WP, Bavari S. 2014. Protection against filovirus diseases by a novel broad-spectrum nucleoside analogue BCX4430. Nature 508:402–405. https://doi.org/10.1038/nature13027.
37. Qiu X, Wong G, Audet J, Bello A, Fernando L, Alimonti JB, Fausther-Bovendo H, Wei H, Aviles J, Hiatt E, Johnson A, Morton J, Swope K, Bohorov O, Bohorova N, Goodman C, Kim D, Pauly MH, Velasco J, Pettitt J, Olinger GG, Whaley K, Xu B, Strong JE, Zeitlin L, Kobinger GP. 2014. Reversion of advanced Ebola virus disease in nonhuman primates with ZMapp. Nature 514:47–53. https://doi.org/10.1038/nature13777.
38. Takashita E, Ejima M, Ogawa R, Fujisaki S, Neumann G, Furuta Y, Kawaoka Y, Tashiro M, Odagiri T. 2016. Antiviral susceptibility of influenza viruses isolated from patients pre- and post-administration of favipiravir. Antiviral Res 132:170–177. https://doi.org/10.1016/j.antiviral.2016.06.007.
39. Delang L, Segura Guerrero N, Tas A, Quérat G, Pastorino B, Froeyen M, Dallmeier K, Jochmans D, Herdewijn P, Bello F, Snijder EJ, de Lamballerie X, Martina B, Neyts J, van Hemert MJ, Leyssen P. 2014. Mutations in the chikungunya virus non-structural proteins cause resistance to favipiravir (T-705), a broad-spectrum antiviral. J Antimicrob Chemother 69:2770–2784. https://doi.org/10.1093/jac/dku209.